Room Temperature Binding of CO to Cobaltous Porphyrin π Cation Radical: Spectroscopic Characterization of Mono and Bis CO Complexes with Cobaltic Porphyrin

Einhard Schmidt,[†] Hong Zhang,[†] Chi K. Chang,[†] Gerald T. Babcock,[†] and W. Anthony Oertling*,[‡]

Contribution from the Department of Chemistry and the LASER Laboratory, Michigan State University, East Lansing, Michigan 48824-1322, and Department of Chemistry/Biochemistry, Mail Stop 74, Eastern Washington University, 526 5th Street, Cheney, Washington 99004-2431

Received March 6, 1995[⊗]

Abstract: When CO(g) is added to solutions of the cobaltous porphyrin π cation radical [Co(II)OEP$^{\bullet}$]ClO_4, prepared by oxidation of CoOEP by $AgClO_4$ in anhydrous CH_2Cl_2, room temperature binding of CO to the metal center occurs. Two distinct products result, [(CO)Co(III)OEP]ClO_4 and [$(CO)_2$Co(III)OEP]ClO_4. These compounds exhibit Soret maxima at 366 and 414 nm, respectively. Resonance Raman (RR) spectra measured before the addition of CO are used to characterize the cobaltous porphyrin π cation radical, and, after the addition of CO, RR spectra obtained by using 363.8 nm excitation confirm the occurrence of the five-coordinate Co(III) porphyrin complex. This complex, along with halide ligated analogs, displays some structure-sensitive vibrational frequencies which suggest that an unusual distortion of the porphyrin core occurs in CH_2Cl_2 solution. RR spectra obtained by using 413.1 nm excitation after the addition of CO are used to identify the second product as a typical six-coordinate cobaltic porphyrin. Titrations with CO reveal that the five- and six-coordinate complexes, [(CO)Co(III)OEP]ClO_4 and [$(CO)_2$Co(III)OEP]ClO_4, form with $P_{1/2}$ values of 36 ± 3 and 4000 ± 300 Torr of CO, respectively. Isosbestic points in the UV−vis spectra occur at 368 nm for binding of the first CO and at 385 nm during binding of the second CO ligand. FTIR and RR spectra of [(CO)Co(III)OEP]ClO_4 reveal vibrations at 2110 and 441 cm^{-1} which shift upon substitution of ^{13}CO or $C^{18}O$ for the natural abundance CO. Isotope sensitive vibrations of [$(CO)_2$Co-(III)OEP]ClO_4 were measured at 2137 and 468 cm^{-1}. In each case the modes above 2100 cm^{-1} correspond to C≡O stretching frequencies, while the lower frequency features are assigned to Co−C stretching motions. The resonance Raman enhancement of these isotope sensitive frequencies confirm CO binding to the metal center. The selective presence of these features in the Raman and FTIR data is consistent with that expected from symmetry based selection rules for five- and six-coordinate CO complexes. The relatively high C≡O stretching frequencies observed are suggestive of weak metal d$\pi \rightarrow$ ligand π^* backbonding that results from the oxidation of Co(II) to Co(III).

Introduction

Synthetic cobalt porphyrin complexes have been used as models for oxygen transport proteins.[1] Low temperature binding of diatomics such as O_2, CO, and NO to conventional cobaltous porphyrins has been achieved,[2] with ligation readily and unambiguously established by vibrational spectroscopy.[3] Binding of dioxygen has received the most attention, and matrix isolation techniques have been used to facilitate these studies.[3] As is typical of diatomic ligands, the O−O stretching frequency is modified by bonding to the metal and can usually be detected by infra red spectroscopy,[4,5] whereas resonance enhancement of the lower frequency Co−O_2 vibrations make these frequencies readily available from Raman measurements.[6,7] Thus, it is useful to use both techniques in order to establish all metal−ligand vibrational frequencies. Vibrational assignments are necessarily verified by isotopic substitutions on the ligand atoms, which affects the vibrational frequencies in these simple systems in a relatively straightforward manner.[8] Use of specialized protected porphyrins allow room temperature Fourier transform infrared (FTIR) and resonance Raman (RR) studies of oxy cobaltous adducts in solution.[9] Possible protein interactions can be modeled, and their effects on vibrational frequencies assessed in this manner.[10] Some interesting studies of vibrational coupling between bound dioxygen vibrations and vibrational modes of trans ligands and solvent have been done with oxy cobaltous porphyrins.[11] Cobalt porphyrins reconstituted into

[†] Michigan State University.

[‡] Eastern Washington University.

[⊗] Abstract published in *Advance ACS Abstracts,* March 1, 1996.

(1) (a) Stynes, D. V.; Stynes, H. C.; James, B. R.; Ibers, J. A. *J. Am. Chem. Soc.* **1973**, *95*, 1796−1801. (b) Jones, R. D.; Summerville, D. A.; Basolo, F. *Chem. Rev.* **1979**, *79*, 139−179. (c) Liu, H.-Y.; Abdalmuhdi, I.; Chang, C. K.; Anson, F. C. *J. Phys. Chem.* **1985**, *89*, 665−670. (d) Collman, J. P.; Zhang, X.; Wong, K.; Brauman, J. I. *J. Am. Chem. Soc.* **1994**, *116*, 6245−6251.

(2) (a) Wayland, B. B.; Mohajer, D. *J. Am. Chem. Soc.* **1971**, *93*, 5295−5296. (b) Wayland, B. B.; Minkiewicz, J. V.; Abd-Elmageed, M. E. *J. Am. Chem. Soc.* **1974**, *96*, 2795−2801. (c) Wayland, B. B.; Mehne, L. F.; Swartz, J. *J. Am. Chem. Soc.* **1978**, *100*, 2379−2149.

(3) Kozuka, M.; Nakamoto, K. *J. Am. Chem. Soc.* **1981**, *103*, 2162−2168.

(4) Urban, M. W.; Nakamoto, K.; Kincaid, J. *Inorg. Chim. Acta* **1982**, *61*, 77−81.

(5) Nakamoto, K.; Paeng, I. R.; Kuroii, T.; Isobe, T.; Oshio, H. *J. Mol. Struct.* **1988**, *189*, 293- 300.

(6) Tsubaki, M.; Yu, N.-T. *Proc. Natl. Acad. Sci. U.S.A.* **1981**, *78*, 3581−3585.

(7) Bajdor, K.; Nakamoto, K; Kincaid, J. *J. Am. Chem. Soc.* **1983**, *105*, 678−679.

(8) For a review, see: Yu, N.-T.; Kerr, E. A. In *Biological Applications of Raman Spectroscopy*; Spiro, T. G., Ed.; 1988; Vol. 3, pp 39−95.

(9) (a) Collman, J. P.; Brauman, J., I.; Halbert, T. R.; Suslick, K. S. *Proc. Natl. Acad. Sci. U.S.A.* **1976**, *73*, 3333−3337. (b) Mackin, H. C.; Tsubaki, M.; Yu, N.-T. *Biophys. J.* **1983**, *41*, 349−357.

(10) (a) Odo, J.; Imai, H.; Kyuno, E.; Nakamoto, K. *J. Am. Chem. Soc.* **1988**, *110*, 742−748. (b) Proniewicz, L. M.; Odo, J.; Góbral, J.; Chang, C. K.; Nakamoto, K. *J. Am. Chem. Soc.* **1989**, *111*, 2105−2110. (c) Proniewicz, L. M.; Bruha, A.; Nakamoto, K.; Kyuno, E.; Kincaid, J. R. *J. Am. Chem. Soc.* **1989**, *111*, 7050−7056.

0002-7863/96/1518-2954$12.00/0

apo-myoglobin and apo-hemoglobin have been characterized by resonance Raman (RR) measurements.[12] Oxy derivatives of reconstituted cobalt myoglobin are stable at room temperature, and RR measurements of these complexes originally revealed the O═O stretching frequency;[6] indeed, the O−O stretching vibration is not easily observed in oxy (Fe) myoglobin by Raman or IR[13] measurements. Thus, many RR studies of oxygen transport proteins have used these oxy cobaltous adducts.[14]

Oxidized derivatives of cobalt porphyrins have been looked upon as models for intermediates in the enzymatic functions of catalases, peroxidases, and cytochromes P_{450}.[15] During the catalysis cycle, the heme cofactors of these enzymes are oxidized by two electrons, i.e., both at the metal center and the porphyrin macrocycle, yielding an oxoferryl porphyrin π cation radical, $[O{=}Fe(IV)P^{\bullet}]^{+}$. Depending on the specific enzyme, the porphyrin cation radical may be subsequently transferred to an amino acid side chain. Like the heme cofactor, cobaltous porphyrins readily lose one electron from each of the metal and the ring macrocycle. In particular, when cobaltous octaethylporphyrin CoOEP is oxidized by two electrons to $[Co(III)OEP^{\bullet}]^{2+}$, two distinct species are possible, one gray and one green in color.[16,17] These two distinct UV−visible absorbance signatures were originally thought to be indicative of the electronic state, $^2A_{1u}$ or $^2A_{2u}$, but later Oertling *et al.*[18] and Sandusky *et al.*[19,20] used Raman, EPR, and ENDOR measurements to demonstrate that the gray and the green $[Co(III)OEP^{\bullet}]^{2+}$ complexes both have a $^2A_{1u}$ ground electronic state. These studies were in accord with earlier interpretations of NMR data[21] and concurrent Raman work by Czernuszewicz *et al.*[22] Our analysis suggested that differences in macrocycle conformation most likely cause variations in the porphyrin N donation to the metal, giving rise to the distinct spectral types.[20] Crystallographers have recently recognized two categories of solid state porphyrin π cation radicals derivatives, one that forms π−π dimers and exhibits S_4-ruffled geometries and another that displays relatively planar conformations.[23] Thus, the gray and the green solution species of $[Co(III)OEP^{\bullet}]^{2+}$ may correspond to these two solid state conformations.

Loss of one electron from CoOEP can result in a number of possible products, depending primarily on the presence of coordinating ligands. Salehi *et al.*[24] showed that one-electron oxidation of this compound by $AgClO_4$ in scrupulously dry CH_2Cl_2 results in ring-centered oxidation yielding a pale, bluish-gray $[Co(II)OEP^{\bullet}]ClO_4$. This complex is sensitive to the presence of even weakly ligating species (e.g., H_2O). Any axial ligand interactions with the Co(II) (a d^7 complex) cause an intramolecular electron transfer from the metal d_{z^2} orbital into the electron deficient ring system. We have observed that reactions of the type

$$[Co(II)OEP^{\bullet}]ClO_4 + L \rightarrow [LCo(III)OEP]ClO_4$$

$$[Co(II)OEP^{\bullet}]ClO_4 + 2L \rightarrow [L_2Co(III)OEP]ClO_4$$

occur very easily.[24,25] These adducts are at the same formal oxidation level yet each has a distinct spectral signature. The cobaltous π cation radical has an absorbance maximum at 377 nm, quite different from either the gray or green cobaltic π cation radicals.[16,25] The five-coordinate cobaltic complex is easily made when L is a halide anion and exhibits two somewhat diffuse optical absorbances at ∼373 and 546 nm, whereas the spectra of six-coordinate complexes display sharper features at ∼410, 525, and 558 nm for fairly weak ligands, with these features shifting to the red as the ligand strength increases.[24,25] It is not uncommon for samples of the one-electron oxidized adduct to display heterogeneity, and many spectra in the literature are due to mixtures of these species.

In contrast to the extensive investigation of dioxygen complexes of cobalt porphyrins described above, there are relatively few reports of carbonmonoxy cobaltous complexes[2,3] and none at room temperature. Kadish and co-workers have recently presented evidence suggesting that CO will bind cobalt porphyrins at room temperature when a one-electron oxidation of a cobaltous TPP (tetraphenylporphyrin) or OEP is carried out electrochemically under a CO atmosphere.[26,27] The result is a cobaltic carbonmonoxy adduct. Preceding the latter work, there was, to our knowledge, only a single report of a cobaltic CO complex,[28] and it is considered somewhat odd for CO to bind metal ions in higher oxidation states due to the π acid nature of the ligand.[29] If oxidation of CoOEP under CO initially produces a cobaltous π cation radical with subsequent CO binding, then CO may simply serve as the ligand L in this case, analogous to the reactions pictured above. In the present work, we prepare $[Co(II)OEP^{\bullet}]ClO_4$ and subsequently introduce CO in a separate step. In agreement with the earlier work,[26,27] we detect formation of cobaltic carbonmonoxy complexes. Here we report conclusive evidence of CO binding to cobalt, namely both Co−CO and CoC≡O stretching frequencies, verified with isotopic substitution. Furthermore, we demonstrate that both five-coordinate $[(CO)Co(III)OEP]ClO_4$ and six-coordinate $[(CO)_2Co(III)OEP]ClO_4$ can be formed with distinct formation equilibrium constants for these species. Our analysis reveals that

(11) (a) Bajdor, K.; Kincaid, J. R.; Nakamoto, K. *J. Am. Chem. Soc.* **1984**, *106*, 7741−7747. (b) Kincaid, J. R.; Proniewicz, L. M.; Bajdor, K.; Bruha, A.; Nakamoto, K. *J. Am. Chem. Soc.* **1985**, *107*, 6775−6781. (c) Proniewicz, L. M.; Kincaid, J. *J. Am. Chem. Soc.* **1990**, *112*, 675−681.

(12) (a) Woodruff, W. H.; Spiro, T. G.; Yonetani, T. *Proc. Natl. Acad. Sci. U.S.A.* **1974**, *71*, 1065−1069. (b) Woodruff, W. H.; Adams, D. H.; Spiro, T. G.;Yonetani, T. *J. Am. Chem. Soc.* **1975**, *97*, 1695−1698

(13) (a) Barlow, C. H.; Maxwell, J. C.; Wallace, W. J.; Caughey, W. S. *Biochem. Biophys. Res. Commun.* **1973**, *55*, 91−95. (b) Potter, W. T.; Tucker, M. P.; Houtchens, R. A.; Caughey, W. S. *Biochemistry* **1987**, *26*, 4699−4707.

(14) (a) Kitagawa, T.; Ondrias, M. R.; Rousseau, D. L.; Ikeda-Saito, M.; Yonetani, T. *Nature* **1982**, *298*, 869−871. (b) Thompson, H. M.; Yu, N.-T.; Gersonde, K. *Biophys J.* **1987**, *87*, 289−295. (c) Bruha, A.; Kincaid, J. R. *J. Am. Chem. Soc.* **1988**, *110*, 6006−6014.

(15) (a) Frew, J. E.; Jones, P. In *Advances in Inorganic and Bioinorganic Mechanism*; Academic Press: New York, 1984; Vol. 3, pp 175−212. (b) Groves, J. T. In *Cytochrome P-450: Structure, Mechanism and Biochemistry;* Ortiz de Montellano, P., Ed.; Plenum Press: New York, 1986; Chapter 1.

(16) Dolphin, D.; Forman, A.; Borg, D. C.; Fajer, J.; Felton, R. H. *Proc. Natl. Acad. Sci. U.S.A.* **1971**, *68*, 614−618.

(17) Fuhrhop, J.-H.; Kadish, K. M.; Davis, D. G. *J. Am. Chem. Soc.* **1973**, *95*, 5140−5147.

(18) Oertling, W. A.; Salehi, A.; Chang, C. K.; Babcock, G. T. *J. Phys. Chem.* **1989**, *93*, 1311- 1319.

(19) Sandusky, P. O.; Salehi, A.; Chang, C. K.; Babcock, G. T. *J. Am. Chem. Soc.* **1989**, *111*, 6431−6439.

(20) Sandusky, P. O.; Oertling, W. A.; Chang, C. K.; Babcock, G. T. *J. Phys. Chem.* **1991**, *95*, 4300−4307.

(21) (a) Morishima, I.; Takamuki, Y.; Shiro, Y. *J. Am. Chem. Soc.* **1984**, *106*, 7666−7672. (b) Godziela, G. M.; Goff, H. M. *J. Am. Chem. Soc.* **1986**, *108*, 2237−2243.

(22) Czernuszewicz, R. S.; Macor, K. A.; Li, X. Y.; Kincaid, J. R.; Spiro, T. G. *J. Am. Chem. Soc.* **1989**, *111*, 3860−3869.

(23) Schulz, C. E.; Song, H.; Lee, Y. J.; Mondal, J. U.; Mohanrao, K.; Reed, C. A.; Walker, F. A.; Scheidt, W. R. *J. Am. Chem Soc.* **1994**, *16*, 7196−7203.

(24) Salehi, A.; Oertling, W. A.; Babcock, G. T.; Chang, C. K. *J. Am. Chem. Soc.* **1986**, *108*, 5630−5631.

(25) Oertling, W. A.; Salehi, A.; Chung, Y. C.; Leroi, G. E.; Chang, C. K.; Babcock, G. T. *J. Phys. Chem.* **1987**, *91*, 5887−5898.

(26) Mu, X. H.; Kadish, K. M. *Inorg. Chem.* **1989**, *28*, 3743−3747.

(27) Hu, Y.; Han, B. C.; Bao, L. Y.; Mu, X. H.; Kadish, K. M. *Inorg. Chem.* **1991**, *30*, 2444- 2446.

(28) Herlinger, A. W.; Brown, T. L. *J. Am. Chem. Soc.* **1971**, *93*, 1790−1791.

(29) Jones, L. H.; McDowell, R. S.; Goldblatt, M. *Inorg. Chem.* **1969**, *11*, 2349−2363.

the earlier work resulted in formation of predominantly the ***bis***-carbonmonoxy derivative, rather than the ***mono***-carbonmonoxy adduct, as was reported.[27]

Experimental Section

Porphyrins were synthesized,[30] and metals were inserted according to established methods.[31] Oxidations were carried out by adding an excess of anhydrous $AgClO_4$(s) to the cobalt porphyrin solution and stirring for 1−3 h in an evacuated cell. CO(g) was typically bubbled into the sample through a syringe, while a second needle was used as a vent to expel excess gas.

For the CO titration, the sample was prepared as described above in dry CH_2Cl_2. CO was introduced with a calibrated gas tight syringe. Before each injection, the pressure within the gas tight syringe was allowed to equilibrate to atmospheric pressure, estimated at 760 Torr. The volume of the titration vessel was 135 mL. Thus, by starting under vacuum and systematically injecting into the vessel a known volume of CO gas, we were able to estimate, using the ideal gas law, the partial pressure of CO at each step in the titration via $(V_{injected}/V_{vessel})$*760 Torr.

FTIR requires highly concentrated samples. Due to the limited solubility of CoOEP in CH_2Cl_2 the necessary concentrations were unattainable. However, 2,4,6,8-tetramethyl-3,7-dioctylporphine-1,5-dimethylpropanoate cobalt(II) (CoC_8P) was sufficiently soluble in CH_2Cl_2 so that FTIR samples could be made. To ensure that CoC_8P had redox and ligation properties similar to those of CoOEP, we used UV−vis absorption spectroscopy to follow the oxidation and CO titration of CoC_8P. FTIR samples were prepared by placing a milligram of cobalt porphyrin and anhydrous $AgClO_4$ into a vial flushed with N_2(g) and sealed with a rubber septum. Freshly distilled methylene chloride (1 mL) was injected into the vial with a Hamilton gas tight syringe. Deuterated solvent was used as supplied by Cambridge Isotope Laboratories. After oxidation was complete, a gas tight syringe was used to transfer the sample into a 0.050 mm NaCl cavity cell sealed with a rubber septum. Carbon monoxide was bubbled into the sample using a gas syringe, while a second needle was used as a vent to expel excess CO. Solution infrared spectra were recorded on a Nicolet IR/42 FTIR spectrometer.

Raman spectra were obtained by using a 90° scattering geometry and were measured with either a Spex 1401 equipped with a PMT or a Spex 1877 monochromator equipped with an OMA III diode array detector. Laser emissions at 363.8 and 413.1 nm were from a Coherent Innova 200 argon ion laser and a Coherent Innova 90 krypton ion laser, respectively. UV−vis absorption spectra, obtained using a Perkin-Elmer Lambda 5 spectrometer, were recorded prior to and following Raman studies to confirm sample integrity. Anaerobic quartz cuvettes were used for both the Raman and UV−vis measurements.

Results

UV−vis absorbance spectra depicting the sequential oxidation and ligand binding of Co(II)OEP are shown in Figure 1. Co(II)OEP (solid line) is oxidized by one-electron in anhydrous CH_2Cl_2 to give the cobaltous π cation radical $[Co(II)OEP^{\bullet}]ClO_4$ (dashed line). The spectrum of this species displays a Soret maxima at 377 nm.[24,25] When gaseous CO is introduced above the solution to a pressure of approximately 1 atm, a split Soret band with maxima at 366 and 414 nm develops, as in Figure 1c (dotted line). Also, typical Q-band absorptions at approximately 528 and 557 nm replace the broad diffuse visible absorptions characteristic of π cation radical, suggesting that the porphyrin ring has regained an electron. The relative intensities of the two absorptions in the split Soret band of Figure 1c are dependent on CO pressure, and titration with CO yields

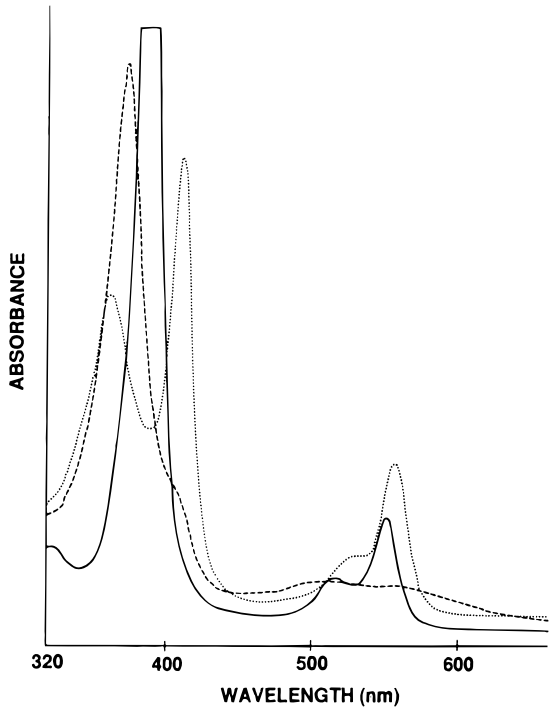

Figure 1. Room temperature UV−visible absorbance spectra of (a) Co(II)OEP in CH_2Cl_2 (—); (b) one-electron oxidized $[Co(II)OEP^{\bullet}]ClO_4$ in CH_2Cl_2 under an N_2 atmosphere (— —); and (c) sample from (b) under a CO atmosphere (•••). The 366 nm Soret maximum corresponds to a mono-carbonmonoxy complex $[(CO)Co(III)OEP]ClO_4$, and the 414 nm Soret maximum corresponds to a bis-carbonmonoxy complex $[(CO)_2Co(III)OEP]ClO_4$.

spectra with well-defined isosbestic points (see below). This suggests that the bands at 366 and 414 nm arise from distinct complexes. Thus, initial oxidation results in a cobaltous π cation radical and subsequent introduction of CO yields two distinct complexes, one with a Soret absorbance maximum of 366 nm and another with an aborbance maximum of 414 nm, that are likely ***not*** porphyrin π cation radicals, as evidenced by their intense visible absorptions.

By using laser lines in resonance with each of the two absorbance maxima, Raman measurements can provide selective enhancement of vibrational spectra from each of the two species giving rise to the Soret absorptions in Figure 1c. We will first discuss spectral resolution of the 366 nm absorbing species. Furthermore, RR spectra of metalloporphyrin π cation radicals are distinct from those of metalloporphyins[18,22,24,25] and can be used to characterize the oxidation and ligation state of these species. The spectrum of $[Co(II)OEP^{\bullet}]ClO_4$, obtained by using 363.8 nm excitation, before CO is introduced, is shown in Figure 2a. After the introduction of CO, use of the 363.8 nm excitation will enhance Raman scattering specific to the 366 nm absorbing complex. Such spectra appear in Figure 2b. Finally, Figure 2c displays the result of a similar experiment in which isotopically labeled ^{13}CO was used rather than natural abundance CO.

The 1300−1700 cm^{-1} region contains several structure-sensitive frequencies that can be used to characterize both the radical and nonradical species involved.[18,22,24,25,31] Table 1 collects these vibrational frequencies and assigns normal modes according to earlier normal coordinate calculations.[32,33] The

(30) (a) Wang, C. B.; Chang, C. K. *Synthesis* **1979**, 548−459. (b) Eaton, S. S.; Eaton, G. R.; Chang, C. K. *J. Am. Chem. Soc.* **1985**, *107*, 3177−3184. (c) Falk, J. E. In *Porphyrins and Metalloporphyrins*; Elsevier: New York, 1964; pp 798.

(31) (a) Li, X.; Spiro, T. G. *J. Am. Chem. Soc.* **1988**, *110*, 6024 −6033. (b) Spiro, T. G.; Czernuszewicz, R. S.; Li, X.-Y. *Coord. Chem. Rev.* **1990**, *100*, 541−571.

(32) Abe, M.; Kitagawa, T.; Kyogoku, Y. *J. Chem. Phys.* **1978**, *69*, 4526−4534.

(33) (a) Li, X.-Y.; Czernuszewicz, R. S.; Kincaid, J. R.; Spiro, T. G. *J. Am. Chem. Soc.* **1989**, *111*, 7012−7023. (b) Li, X.-Y.; Czernuszewicz, R. S.; Kincaid, J. R.; Stein, P.; Spiro, T. G. *J. Phys. Chem.* **1990**, *94*, 47−61.

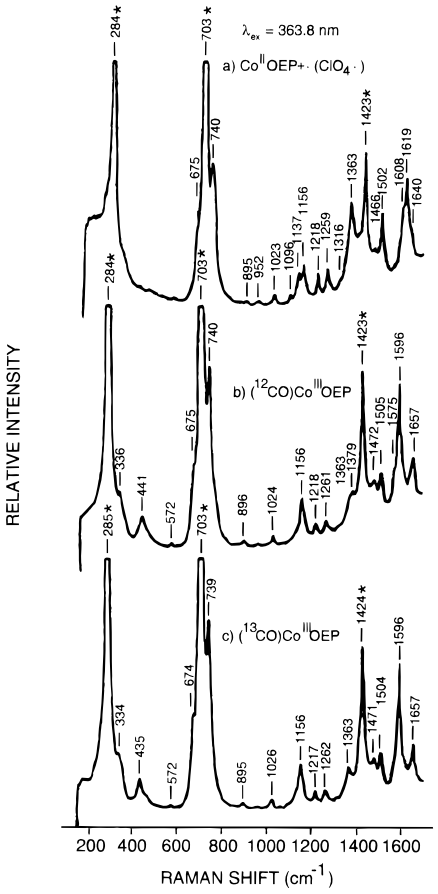

Figure 2. Resonance Raman spectra of one-electron oxidized species obtained at room temperature using 5 mW of 363.8 nm laser excitation. The samples were prepared in dry CH_2Cl_2 as described in the Experimental Section; UV−vis spectra were monitored prior to and following the Raman measurement to verify the integrity of the samples. Sample (a) was under air and consisted of [Co(II)OEP•]ClO_4. Samples (b) and (c) were under carbon monoxide as indicated. Laser excitation at this wavelength will select for the mono-carbonmonoxy complex [(CO)Co(III)OEP]ClO_4 as described in the text. [Sample (c) contains a small amount of residual starting material, [Co(II)OEP•]ClO_4, as evidenced by the RR intensity at 1363 cm^{-1}.]

Table 1. Structural Sensitive Vibrational Frequencies (cm^{-1}) Observed in Resonance Raman Spectra Obtained at the Given Excitation Wavelengths (nm)

			[$(CO)_n$Co(III)OEP]ClO_4	
normal mode	Co(II)OEP 363.8 nm	[Co(II)OEP•]ClO_4 363.8 nm	363.8 nm $n = 1$	413.1 nm $n = 2$
ν_4 (C_aN)	1379	1363	1379	1376
ν_3 (C_aC_m)	1512	1502	1505	1513
ν_{11} (C_bC_b)	1575	1608	1575	1571
ν_2 (C_bC_b)	1599	1619	1596	1592
ν_{10} (C_aC_m)	1647	1640	1657	1647

first column in the table gives characteristic frequencies for the CoOEP (spectra not shown). The second column reflects frequencies obtained from Figure 2a. These Raman frequencies, together with the 377 nm absorbance maximum, are indicative of a "gray type" cobaltous π cation radical,[24,25] which is the starting material for our present experiments. The third column contains Raman frequencies in this structure-sensitive region obtained from Figure 2b,c for the 366 nm absorbing species in the final mixture. The frequencies listed in Table 1 for this compound are quite similar to those of [BrCo(III)OEP],[25] a rather unique five-coordinate cobaltic compound which also displays a dramatically blue-shifted Soret absorbance (373 nm).

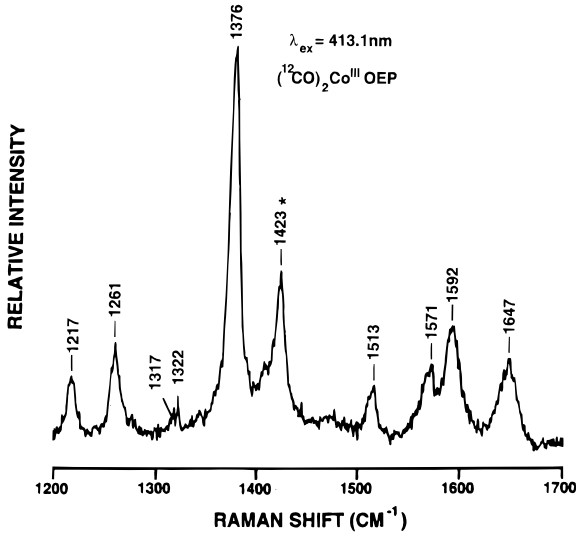

Figure 3. Resonance Raman spectrum of one-electron oxidized species under carbon monoxide obtained at room temperature using 5 mW of 413.1 nm laser excitation. Laser excitation at this wavelength will select for the bis-carbonmonoxy complex [$(CO)_2$Co(III)OEP]ClO_4 as described in the text. Sample integrity was monitored as described in Figure 2.

This suggests that the 366 nm absorbing species is similarly a five-coordinate cobaltic adduct, as is discussed in detail below.

Evidence for ligation of CO in this five-coordinate complex results from comparison of Figure 2 (parts b and c). Aside from the small contribution at 1363 cm^{-1} in Figure 2c from some residual cobaltous π cation radical in the sample under ^{13}CO atmosphere, comparison of Figure 2 (parts b and c) suggests that only one vibration is affected by the isotopic substitution: the low frequency feature at 441 is shifted to 435 cm^{-1} in the ^{13}CO sample. Thus, this feature corresponds to a cobalt−CO vibration, unambiguously establishing CO binding to the metal center.

RR spectra obtained by using 413.1 nm laser excitation of the sample under carbon monoxide should select for contributions from the 414 nm chromophore. These appear in Figure 3 and give rise to the frequencies listed in the last column of Table 1. These frequencies are very similar to those of the starting material, CoOEP. Together with the red-shifted Soret maximum at 414 nm, these are consistent with a six-coordinate cobaltic complex, $(L)_2$Co(III)OEP.[12,25] The spectrum obtained by using $\lambda_{ex} = 413.1$ nm in Figure 3 is distinct from that observed with $\lambda_{ex} = 363.8$ nm (Figure 2b) indicating that efficient spectral resolution of the two species resulting from CO ligation has been achieved.

Evidence for CO ligation in the six-coordinate sample appear in Figure 4. This figure displays the low-frequency region of the resonance Raman spectrum obtained by using $\lambda_{ex} = 413.1$ nm and reveals a feature at 468 cm^{-1} that shifts to 461 cm^{-1} in the spectrum of the isotopically labeled ^{13}CO adduct. This frequency is quite different from the analogous one observed with $\lambda_{ex} = 363.8$ nm, which occurs at 441 cm^{-1} and shifts to 435 cm^{-1} when ^{13}CO is used (Figure 2 (parts b and c), above).

The data presented thus far suggest that upon introduction of CO to the cobaltous π cation radical, two species with UV−vis and RR spectra consistent with five- and six-coordinate cobaltic complexes are formed. Low frequency RR spectra of isotopically labeled samples show that both the five- and six-coordinate complexes have CO bound to the metal center. Each complex gives rise to a distinct Co−CO stretching frequency. Because the six-coordinate complex is formed from the five-coordinate complex via addition of CO, it is reasonably

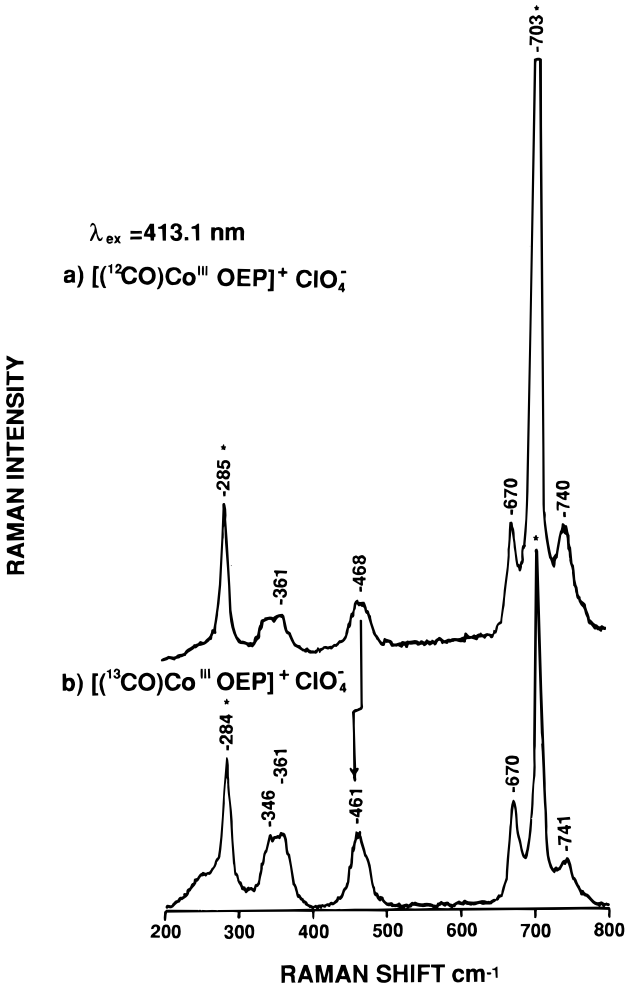

Figure 4. RR spectra obtained under the same conditions as Figure 3.

described as a bis-carbonmonoxy adduct. To confirm this analysis we present below RR and FTIR data revealing additional isotope sensitive vibrations from each of the two product species as well as UV−vis spectra monitoring titration of [Co(II)OEP•]ClO_4 with CO.

Because CO is bound to the chromophores, the RR spectrum may reveal high frequency vibrations corresponding to the C≡O stretching vibrations of the bound ligand. Figure 5 shows the high frequency region of Raman scattering enhanced at λ_{ex} = 363.8 nm. A feature at 2110 cm^{-1} shifts to 2059 cm^{-1} when the isotopically labeled ^{13}CO is used. This is attributed to the five-coordinate species that absorbs at 366 nm. In search of an analogous isotope sensitive band from the six-coordinate species absorbing at 414 nm, we scanned the high frequency region of the scattering resulting from the 413.1 nm laser line but could not detect such a feature.

Solution FTIR spectra (not shown) of analogous samples (see Experimental Section for details of preparation) in both CH_2Cl_2 and CD_2Cl_2 reveal two bands in the C≡O stretching region at 2110 and 2137 cm^{-1}. When the sample is prepared with ^{13}CO, bands are observed at 2061 and 2088 cm^{-1}. The 2110 cm^{-1} feature shifting to 2061 cm^{-1} upon isotopic substitution is in good agreement with the 363.8 nm Raman result (Figure 5) and suggests that this feature arises from the five-coordinate complex. It is then reasonable to assume that the other feature at 2137 shifting to 2088 cm^{-1} upon isotopic substitution, arises from the six-coordinate species. This assumption is consistent with more extensive vibrational analysis presented below.

Absorbance spectra monitoring titration of [Co(II)OEP•]ClO_4 with CO appear in Figure 6. The most intense feature in the

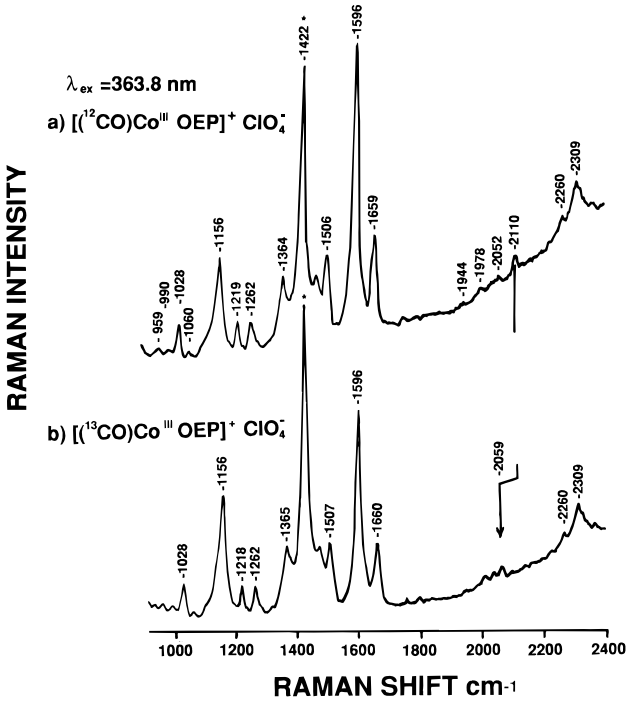

Figure 5. RR spectra obtained under the same conditions as Figure 2.

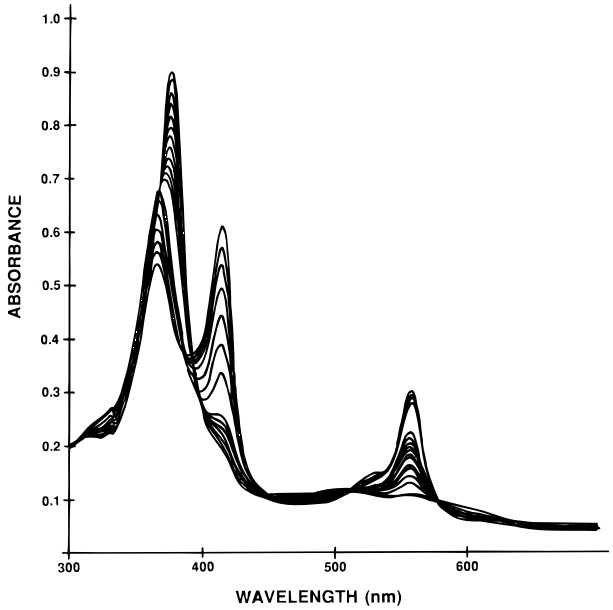

Figure 6. UV−visible spectra obtained during titration of [Co(II)-OEP•]ClO_4 (λ_{max} = 377 nm) with carbon monoxide gas as described in the Experimental Section. Initially the 366 and 555 nm bands increase as the 377 nm band decreases. Further addition of CO causes the 414 nm band to increase at the expense of the 366 nm feature. Concomitant with the latter changes, the 555 nm band diminishes and shifts to 558 nm as a feature at 527 nm is resolved. See text for further details and interpretation.

Soret region (377 nm) originates from the starting material, cobaltous π cation radical. Initially this band diminishes as the band at 366 nm grows, giving rise to an isosbestic point at approximately 368 nm. Concomitant with these changes, a band at 555 nm appears and intensifies along with the 366 nm absorbance. Eventually, with further addition of CO, a feature at 414 nm intensifies as the band at 366 nm diminishes, giving rise to an isosbestic point at about 385 nm. Changes in the Q-band region which accompany the latter spectral change are more subtle, but the band at 555 nm diminishes in intensity and red-shifts slightly to 558 nm and the feature at 527 nm

begins to resolve. The two clearly defined isosbestic points provide credibility for our suggestion of two ligation events. Thus, the pressure dependence of the absorbance spectra suggests the formation of two complexes that are in equilibrium as shown by the following:

$$\underset{377\text{ nm}}{[\text{Co(II)OEP}^{\bullet}]\text{ClO}_4} + \text{CO} \rightleftharpoons \underset{366,\ 555\text{ nm}}{[(\text{CO})\text{Co(III)OEP}]\text{ClO}_4} \quad (1)$$

$$\underset{366,\ 555\text{ nm}}{[(\text{CO})\text{Co(III)OEP}]\text{ClO}_4} + \text{CO} \rightleftharpoons \underset{414,\ 527,\ 558\text{ nm}}{[(\text{CO})_2\text{Co(III)OEP}]\text{ClO}_4} \quad (2)$$

$$[\text{Co(II)OEP}^{\bullet}]\text{ClO}_4 + 2\text{CO} \rightleftharpoons [(\text{CO})_2\text{Co(III)OEP}]\text{ClO}_4 \quad (3)$$

We show below that the equilibrium constant for reaction 3 is very small, making this process negligible. Vibrational analysis of the cobalt−carbonmonoxy vibrations provides further evidence for this scheme and is also presented below, followed by determination of the equilibrium constants for (1)−(3).

Discussion

Analysis of Cobalt−CO Vibrations. The five-coordinate complex $[(CO)Co(III)OEP]ClO_4$ belongs to the C_{4v} point group and a linear Co−C≡O unit is expected to give rise to four vibrations given by $2A_1 + E$. The two vibrations of A_1 symmetry are totally symmetric stretching motions while the E vibrations are a degenerate pair of linear bends. All vibrations are expected to be both Raman and IR active.[34] The linear bends, being degenerate, should occur at the same frequency in the 200−600 cm^{-1} region. One stretch is expected to be primarily νC≡O (occurring at approximately 2000 cm^{-1} or above) and the other νCo−C (occurring in the 300−600 cm^{-1} range). There is little mixing of these stretching coordinates because of the large difference in frequencies.

The six-coordinate complex $[(CO)_2Co(III)OEP]ClO_4$ most likely belongs to the D_{4h} group. A linear O≡C−Co−C≡O unit is expected to generate ten vibrations given by $2A_{1g} + 2A_{2u} + 2E_g + E_u$. The A type modes are stretches, and the E type modes are degenerate linear bends. Gerade vibrations are Raman active, and ungerade vibrations are IR active.[34] The frequency regions in which the vibrations are expected are similar to the C_{4v} case above. For example, a totally symmetric (A_{1g}) Raman active mode ←O≡CCoC≡O→ is expected in the high frequencies, while another, corresponding to symmetric stretching of the metal−carbon bonds ←OC−Co−CO→, is expected in the low frequencies. The situation is similar for IR active A_{2u} antisymmetric stretching modes.

Table 2 collects the observed metal−ligand vibrational frequencies and our vibrational normal mode assignments for axial ligand vibrations of both the five and six-coordinate complexes. Three carbon monoxide isotopomers have been utilized for most of the measurements. The appearance of the 2110 cm^{-1} vibration in both the RR and FTIR data is further support for the formation of the five-coordinate C_{4v} complex. The assignment of the other high frequency FTIR feature at 2137 cm^{-1} to the expected IR active A_{2u} C≡O stretch of the six-coordinate complex is reasonable. The predominance of IR absorbance of solvent, cell, and optics in the low frequency region precluded search for other IR allowed vibrations. RR spectra obtained using 413.1 nm excitation selectively enhances contributions from the six-coordinate complex. In the low frequency region, we were able to easily observe the A_{1g} Co−C stretching frequency at 468 cm^{-1}. The absence of detectable signal from the A_{1g} symmetric C≡O stretch for the six-coordinate species in the high frequency Raman scattering obtained by using 413.1 nm excitation is not totally unexpected because not only is the resonance enhancement of these modes typically much weaker than that of the Co−C stretch but also Raman intensity is proportional to the fourth power of the absolute scattered frequency making detection of this mode by using 413.1 nm excitation (data not shown) more difficult than by using 363.8 nm excitation (Figure 5). The absence of features attributable to bending vibrations is common. Based on the number of d electrons in the metal (6) and the number of π^* electrons in the ligand (0), the geometry of the Co(III)−C≡O is expected to be linear.[8] Yu *et al.*[35] report no RR enhancement of metal−ligand bending vibrations for complexes known to have linear M−C−O geometries. Similarly, because we observed no bending motions in the low frequency RR spectra, CO possibly binds to Co in a linear fashion in these complexes.

Table 2. Observed Frequencies (cm^{-1}) and Normal Mode Assignments of Cobalt-Carbonmonoxy Vibrations for Five- and Six-Coordinate $[(CO)_nCo(III)OEP]ClO_4$ Complexes

mode	[symmetry]	frequency (cm^{-1}) CO	^{13}CO	$C^{18}O$	method of measurement
Five-Coordinate Complex: $2A_1 + E$					
ν(C═O)	[A_1]	2110	2060	2076	RR (363.8 nm), FTIR
ν(Co−C)	[A_1]	441	435	*a*	RR (363.8 nm)
Six-Coordinate Complex: $2A_{1g} + 2A_{2u} + 2E_g + E_u$					
ν_{as}(O═CCoC═O)	[A_{2u}]	2137	2088	2089	FTIR
ν_s(OC−Co−CO)	[A_{1g}]	468	461	*a*	RR (413.1 nm)

[a] We did not attempt to observe the vibration.

The C≡O stretching frequency observed at 2137 cm^{-1} for the six-coordinate and 2110 cm^{-1} for the five-coordinate complex, reflect relatively weak metal dπ → ligand π^* backbonding. This reflects the decreased electron density at the Co(III) due to the high oxidation state. Metals in lower oxidation states are able to donate electrons back into the π^* orbital of the ligand more strongly, causing a greater decrease in the C≡O stretching frequency.[36] For example, C≡O frequencies (cm^{-1}) observed for some M(II) porphyrin complexes include $(CO)_2$CoTPP, 2078; $(CO)_2$FeTPP, 2042; and $(CO)_2$RuTPP, 2005.[3] The 2137 cm^{-1} that we observe for $[CO)_2$-Co(III)OEP]ClO_4 is hardly lowered from the frequency of free CO ~2155 cm^{-1}, indicating that the bonding interaction is dominated by σ donation from the ligand to the metal in this M(III) complex. Although this has not been reported for a CO complex before, it is quite common for analogous CN^- complexes. M^{3+} cyano complexes typically exhibit C≡N stretching frequencies ~2130 cm^{-1}, higher that of free CN^-, ~2080 cm^{-1}, while the νCN frequency in M^{2+} complexes is often lower, ~2050 cm^{-1}.[36] Judging from our observed frequencies, the backbonding in the six-coordinate complex is even weaker than in the five-coordinate complex because in the six-coordinate complex the metal donation must be split between two ligands. Comparison of the C≡O frequency for $(CO)_2$FeTPP, 2042 cm^{-1}, to that of (CO)FeTPP, 1973 cm^{-1}, illustrates the same trend.[2c]

Calculation of Equilibrium Constants and $P_{1/2}$ Values for Reactions 1−3. Assuming Henry's law relating the partial pressure of a gas above a solution to its solution concentration,

(34) Harris, D. C.; Bertolucci, M. D. In *Symmetry and Spectroscopy*; Dover, 1989; pp 93−224.

(35) Yu, N.-T.; Kerr, E. A.; Ward, B.; Chang, C. K. *Biochemistry* **1983**, *22*, 4534−4540.

(36) Nakamoto, K. In *Infrared and Raman Spectra of Inorganic and Coordination Compounds*, 4th ed.; Wiley: 1986; pp 291−308.

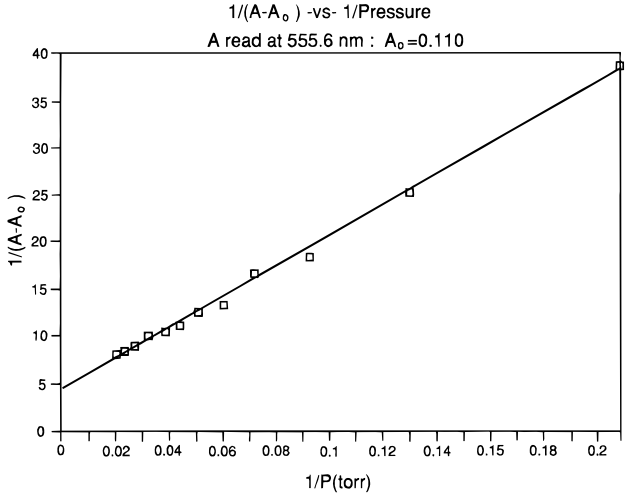

Figure 7. Determination of K_1: Plot of $1/(A - A_0)$ vs 1/pressure (CO). $A_0 = 0.110$. Readings of A and A_0 are at 555.6 nm and correspond to the mono-carbonmonoxy complex. At these pressures contributions from the bis-carbonmonoxy complex and starting material [Co(II)OEP$^{\bullet}$]-ClO_4 were both negligible.

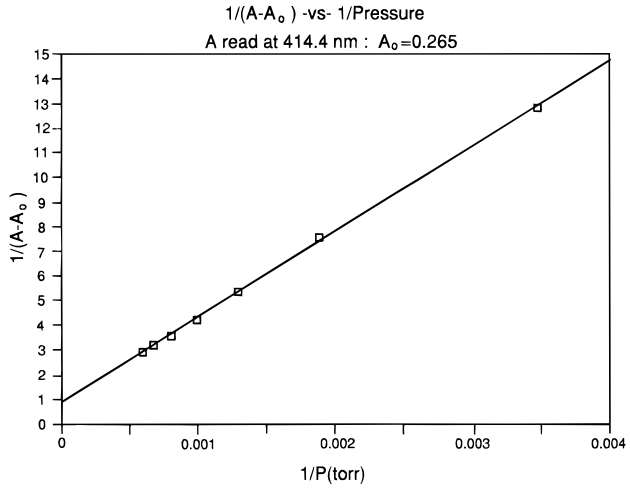

Figure 8. Determination of K_2: Plot of $1/(A - A_0)$ vs 1/pressure (CO). $A_0 = 0.265$. Readings of A and A_0 are at 414.4 nm are due nearly exclusively to the bis-carbonmonoxy complex.

we can write equilibrium constant expressions for (1) and (2):

$$K_1 = \frac{[[(CO)Co(III)OEP]^+]}{[[Co(II)OEP^{\bullet}]^+]P_{CO}}$$

$$K_2 = \frac{[[(CO)_2Co(III)OEP]^+]}{[[(CO)Co(III)OEP]^+]P_{CO}}$$

The true concentration equilibrium constants can be obtained by multiplication of K_1 and K_2 by the appropriate Henry's constant for CO in CH_2Cl_2. K_3 (for the third reaction, above) is the product K_1K_2 and is significant only if $K_2 > K_1$. K_1 and K_2 are determined from Figures 7 and 8 by using the following[37]:

$$\frac{1}{A - A_0} = \frac{1}{K_i(A_\infty - A_0)}\frac{1}{P_{CO}} + \frac{1}{(A_\infty - A_0)}$$

where A represents the absorbance of the system at a particular partial pressure of CO, A_0 is the initial absorbance of the reactant species, K_i is K_1 or K_2, A_∞ is the final absorbance of pure product species, and P_{CO} is the partial pressure of CO. Thus, a plot of $1/(A - A_0)$ vs $1/P_{CO}$ will give a line. A_∞ is determined from the intercept and K_i from the slope. Because only negligible formation of the six-coordinate complex occurs before reaction 1 has gone to completion, we can use the expression above to determine either K_1 or K_2.[38] Figures 7 and 8 show such plots for reactions 1 and 2, respectively. $P_{1/2}$, the pressure of CO when the reaction has proceeded halfway, is given by the reciprocal of the equilibrium constant, $P_{1/2} = (K_i)^{-1}$. From Figures 7 and 8 we obtain $P_{1/2}$ estimates of 36 ± 3 and 4000 ± 300 Torr for reactions 1 and 2, respectively.

Comparison of [(CO)Co(III)OEP]ClO_4 to BrCo(III)OEP and Other Complexes. The UV−vis absorbance spectrum of [(CO)Co(III)OEP]ClO_4 is similar to that of BrCo(III)OEP.[24] Both display dramatically blue-shifted Soret absorbances (366 and 373 nm, respectively, in CH_2Cl_2) compared to that of typical metalloporphyrin complexes. ClCo(III)OEP and ICo(III)OEP also display this blue-shifted Soret maximum;[39] however, we are aware of few other metalloporphyrins with this peculiar spectral signature. The ∼370 nm Soret band is odd in two regards. First, oxidation of Co(II) to Co(III) normally causes a red-shift in porphyrin compounds.[40] (This is of course different for ***iron*** porphyrin complexes, which are not germane to the discussion of this topic.) Thus, the Soret maximum of cobaltic OEP compounds are expected to be red-shifted relative to that of Co(II)OEP (391 nm), as are the Soret absorbances of the six-coordinate adducts. Second, in the absence of spin or oxidation-state changes,[41] ligation of a single axial ligand normally causes a red-shift in the spectrum of the metalloporphyrin, with a second ligand simply causing an additional red-shift. For example, spectral changes of Cu(II) porphyrins[42] upon ligation display the typical red-shifted trend. Indeed, this is what Kadish and co-workers[27] observed for Co(III)TPP$^+$ (TPP = tetraphenylporphyrin) complexes upon sequential ligation of CH_3CN. Thus, the formation of this five-coordinate complex displaying the ***blue***-shifted Soret band appears to be unique to cobaltic complexes of specific porphyrins in solution. Interestingly, (CN)Co(III)OEP is reported to exhibit distinct Soret maxima at 372 and 421 nm,[43] while (CN)Co(III)protoporphyrin IX reconstituted in horseradish peroxidase displays a Soret maximum at 436 nm.[44] The 372 and 421 nm maxima may represent two different conformations of the five-coordinate cobaltic cyano complex. In this interpretation, the 372 nm band most likely arises from this rather unique configuration and the 421 nm band from a more conventional geometry. The 436 nm maximum in the enzyme active site represents the effect of a sixth ligand (histidine, and possibly other influences) from the protein.

It is well-known that RR frequencies are much more informative of structural properties of metalloporphyrins[35] than

(37) Neya, S.; Morishima, I.; Yonezawa, T. *Biochemistry* **1981**, *20*, 2610−1614.

(38) (a) Antonini, E.; Brunori, M. Hemoglobin and Myoglobin and their Reactions with Ligands. In *Frontiers of Biology*; Neuberger, A., Tatum, E. L., Eds.; North Holland Publishing: 1971; Vol. 21. (b) James, B. In *The Porphyrins*; Dolphin, D., Ed.; Academic: New York, 1979; Vol. V, Chapter 6.

(39) Salehi, A. Ph.D. Dissertation, Michigan State University, 1988; pp 143−155.

(40) (a) Tsutsui, M.; Velapoldi, R. A.; Hoffman, L.; Suzuki, K.; Ferrari, A. *J. Am. Chem. Soc.* **1969**, *91*, 3337−3341. (b) Whitten, D. G.; Baker, E. W.; Corwin, A. H. *J. Org. Chem.* **1963**, *28*, 2363−2368.

(41) Kim, D.; Su, O. Y.; Spiro, T. G. *Inorg. Chem.* **1986**, *25*, 3988−3993.

(42) Shelnutt, J. A.; Straub, K. D.; Rentzepis, P. M.; Gouterman, M.; Davidson, E. R. *Biochemistry* **1984**, *23*, 3946−3954.

(43) Tait, C. D.; Holten, D.; Gouterman, M. *J. Am. Chem. Soc.* **1984**, *106*, 6653−6659.

(44) Wang, M.-Y. R.; Hoffman, B. M. *J. Am. Chem. Soc.* **1984,** *106*, 4235−4240.

UV−vis absorbance maxima. Spaulding *et al.*[45] first recognized the linear correlation between the frequency of ν_{19}, an anomalously polarized (ap) mode, and the porphyrin center-to-nitrogen distance. Similar correlations were demonstrated for virtually all high frequency vibrations.[46−48] Metalloporphyrins exhibiting ruffled or domed geometries, for example, ferrous complexes were shown to display ν_{10} and ν_{19} frequencies which were significantly lower than expected from their core sizes.[45−48] Not surprisingly, BrCoOEP was noted to display Raman frequencies that uniquely deviated from these correlations. The BrCoOEP frequencies most sensitive to core-size are 1657 (ν_{10}), 1599 (ν_2), 1575 (ν_{11}), 1572 (ν_{19}), and 1514 (ν_3). In particular, the difference in the ν_{10} (dp) and ν_{19} frequency of metalloporphyrins is typically 54 ± 4 cm^{-1}, whereas in BrCoOEP it is 82 cm^{-1}.[45,25] Comparison of the spectra of Co(II)OEP and BrCo(III)OEP and $[(MeOH)_2Co(III)OEP]Br$[25] reveals that the RR frequencies between 1300 and 1700 cm^{-1} are very similar for the three complexes, with the exception of ν_{10} and ν_{19}. In the spectra of BrCo(III)OEP the ν_{10} frequency is elevated and the ν_{19} frequency lowered from typical values. We have speculated that this results from a severe structural perturbation in solution,[25] and doming of the porphyrin with the metal ion significantly out of the plane has been suggested.[45,49] Recent X-ray crystallographic studies of five-coordinate cobaltous and cobaltic porphyrins reveal Co displacement of 0.1 Å for all derivatives, with porphyrin core geometries for these compounds being either flat or S_4 ruffled.[50] Still the ***elevation*** of ν_{10} displayed by these peculiar five-coordinate complexes is puzzling, however, as both ruffling and doming distortions are expected to ***lower*** both of these frequencies by ∼15 cm^{-1}.[48] We have not been able to obtain crystals of this compound suitable for X-ray crystallography.

Although the ν_3 frequency for the five-coordinate $[(CO)Co(III)OEP]ClO_4$ is somewhat less than that of BrCoOEP, the similarity of the other vibrational frequencies and the Soret maxima of these two complexes attests to shared structural features. We have noted[25] that a μ-nitrido dimer $(OEPFe)_2N$ displays some similar spectral features[51] to that of the bromide complex and have speculated that the severely ruffled porphyrin core and 0.3 Å out-of-plane displacement of Fe in this complex[52] may model the Co(III) complexes studied here.

Another possible cause of a blue-shifted Soret absorbance is aggregation. Shelnutt *et al.*[53] have pointed out that aggregates of some metallouroporphyrins display blue-shifted Soret absorbances similar to those we report. However, our dilution studies show no concentration dependence of the Soret absorbance of BrCoOEP, as would be expected for a dimer or aggregate. At any rate, the solution structure of these five-coordinate Co(III) complexes most likely involves some distorted porphyrin conformation. This conformation perhaps makes the ligation of the sixth ligand more difficult, keeping the equilibrium constant K_2 relatively low.

Acknowledgment. We thank Drs. A. Salehi and W. H. Woodruff for discussion. We also thank Prof. Y. Kim for performing normal coordinate calculations and discussion. This work was supported by NIH Grants GM36520 (to C.K.C.), GM25480 (to G.T.B.), and Northwest Institute for Advanced Study and EWU Foundation grants (to W.A.O), and ACS-PRF# 29543-GB4 grant (to W.A.O.).

JA950744Q

(45) Spaulding, L. D.; Chang, C. C.; Yu, N.-T.; Felton, R. H. *J. Am. Chem. Soc.* **1975**, *97*, 2517−2525.
(46) Callahan, P. M.; Babcock, G. T. *Biochemistry* **1981**, *20*, 952−958.
(47) (a) Parthasarathi, N.; Hansen, C.; Yamaguchi, S.; Spiro, T. G. *J. Am. Chem. Soc.* **1987,** *109*, 3856−3871. (b) Sarma, Y. A. *Spectrochimca Acta* **1989**, 45A, 649−652.
(48) Prendergast, K.; Spiro, T. G. *J. Am. Chem. Soc.* **1992,** *114*, 3793−3801.
(49) Felton, R. H.; Yu, N.-T.; O'Shea, D. C.; Shelnutt, J. A. *J. Am. Chem. Soc.* **1974,** *96*, 3675- 3676.
(50) Summers, J. S.; Petersen, J. L.; Stolzenberg, A. M. *J Am. Chem. Soc.* **1994**, *116*, 7189- 7195.
(51) Hofmann, J. A.; Bocian, D. F. *J. Phys. Chem.* **1984**, *88*, 1472−1479.
(52) Scheidt, W. R.; Summerville, D. A.; Cohen, I. A. *J. Am. Chem. Soc.* **1976,** *96*, 6623−6628.
(53) Shelnutt, J. A.; Dobry, M. M.; Satterlee, J. D. *J. Phys. Chem.* **1984**, *88*, 4980−4987.